
Do Not Let Low-Probability Tokens Over-Dominate in RL for LLMs

Zhihe Yang¹ Xufang Luo^{2*} Zilong Wang² Dongqi Han²
Zhiyuan He² Dongsheng Li² Yunjian Xu^{1*}

¹The Chinese University of Hong Kong, Hong Kong SAR, China.

²Microsoft Research Asia, Shanghai, China.

Abstract

Reinforcement learning (RL) has become a cornerstone for enhancing the reasoning capabilities of large language models (LLMs), with recent innovations such as Group Relative Policy Optimization (GRPO) demonstrating exceptional effectiveness. In this study, we identify a critical yet underexplored issue in RL training: low-probability tokens disproportionately influence model updates due to their large gradient magnitudes. This dominance hinders the effective learning of high-probability tokens, whose gradients are essential for LLMs’ performance but are substantially suppressed. To mitigate this interference, we propose two novel methods: *Advantage Reweighting* and *Low-Probability Token Isolation (Lopti)*, both of which effectively attenuate gradients from low-probability tokens while emphasizing parameter updates driven by high-probability tokens. Our approaches promote balanced updates across tokens with varying probabilities, thereby enhancing the efficiency of RL training. Experimental results demonstrate that they substantially improve the performance of GRPO-trained LLMs, achieving up to a 46.2% improvement in K&K Logic Puzzle reasoning tasks.[†]

1 Introduction

The reasoning capabilities of large language models (LLMs) have recently achieved a milestone breakthrough with the integration of reinforcement learning (RL) during post-training phase [1, 2, 3]. Intuitively, the vast vocabulary size and the auto-regressive generation mechanism of LLMs pose significant challenges for effective exploration due to the exponentially large state space. DeepSeek-R1 [2] eliminates this bias, demonstrating that ‘simple RL with rule-based reward’ can significantly enhance the reasoning abilities of LLMs without relying on scaffolding techniques such as Monte Carlo Tree Search (MCTS) [4, 5] or Progress Reward Modeling (PRM) [6, 7]. Moreover, they introduce a novel algorithm, Group Relative Policy Optimization (GRPO) [8], which has proven highly effective in the domains of mathematics and code, inspiring numerous follow-up studies.

Yu et al. [9] and Liu et al. [10] consistently report that GRPO training leads to progressively longer response lengths, while the increase does not correspond to a proportional improvement in the model’s performance. They attribute this trend to the bias in update weights related to response length inherent in GRPO’s objective. Xiong et al. [11] conduct comparison between GRPO and Proximal Policy Optimization (PPO). They find that the instability of PPO, compared to GRPO, arises from its unnecessary bias toward entirely incorrect responses on overly difficult prompts. In contrast, GRPO mitigates this issue by discarding such prompts through a within-prompt normalization operation. These findings highlight the substantial impact of update bias on training outcomes.

*Corresponding authors.

[†]Our implementation is available at <https://github.com/zhyang2226/AR-Lopti>.

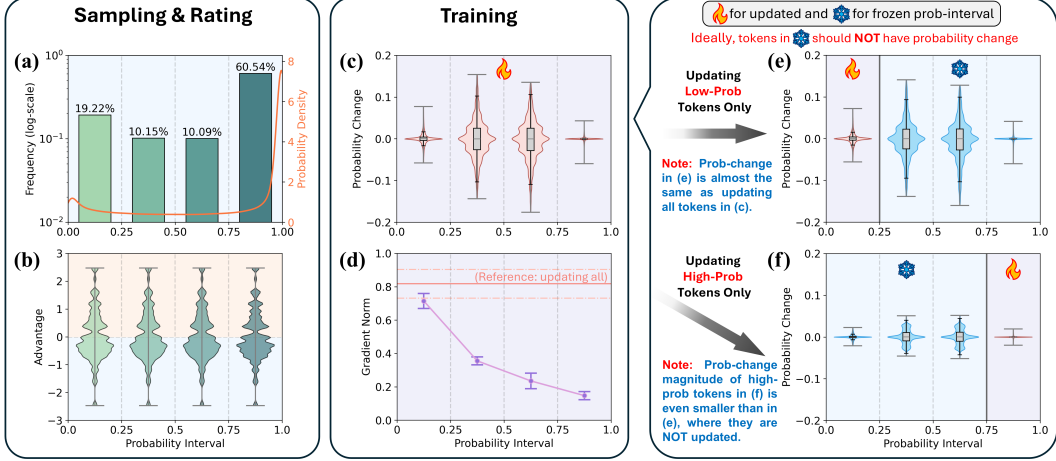


Figure 1: Experimental analysis on the K&K Logic Puzzle dataset during GRPO training of Qwen2.5-7B-Instruct-1M. Tokens are divided into four groups based on probability quartiles. (a) Token probability distribution and (b) corresponding advantages. (c) Token probability changes after updates (using SGD with $\text{lr}=1\text{e-}3$) and (d) gradient norms for each probability group. Effects of selective updates: (e) Probability changes when only tokens in the lowest quartile (probability < 0.25) are updated, and (f) when only tokens in the highest quartile (probability > 0.75) are updated. To ensure clarity, the top 1% of outlier samples in the violin plots for token probability changes are excluded. Results are averaged over 10 randomly sampled batches.

In this study, we identify another important source of update bias in RL training, which is orthogonal to aforementioned ones and has rarely been noted in prior research. This bias arises from the gradient perspective and is strongly correlated with the token probabilities. As shown in Figure 1, during GRPO training, tokens are divided into four groups based on probability quartiles. The policy gradient is conducted with the advantage presented in Figure 1(b). Figure 1(d) shows that low-probability tokens generate disproportionately larger gradients compared to high-probability ones. Since each RL update involves hundreds of thousands of tokens with interacting gradients, low-probability tokens are expected to have a greater influence. To verify this, we independently update tokens from the lowest and highest quartiles, as shown in Figures 1(e) and (f). The pattern in (e) closely matches (c), while (f) looks significantly different. Interestingly, in (e), even though high-probability tokens were not updated, their probabilities changed more significantly than when they were updated (as shown in (f)). Thus, we conclude that **low-probability tokens dominate model updates** during RL training and that **this dominance may impede the precise adjustment of the probability distribution across all tokens**. Notably, we observe that high-probability tokens are much less likely to be updated in the correct direction compared to low-probability tokens (cf. Figure 3).

By deriving the gradients induced by individual tokens, we reveal a key property of RL training that explains the phenomenon illustrated in Figure 1. Specifically, for an LLM comprising a benign neural network, the gradient norm of any intermediate activation corresponding to a single token is bounded between two values proportional to $(1 - \pi)$, where π is the token’s probability. This property underscores that tokens with lower probabilities result in larger gradient magnitudes, whereas tokens with probabilities approaching 1 yield gradients that are nearly negligible.

To mitigate the over-dominance of low-probability tokens and promote more efficient updates, we propose two simple yet effective methods: *Advantage Reweighting*, which reduces the weight assigned to low-probability tokens, and *Low-Probability Token Isolation (Lopti)*, which separates low-probability tokens and updates them prior to high-probability tokens. Both methods attenuate gradients from low-probability tokens while emphasizing parameter updates driven by high-probability tokens. Notably, the first one incurs almost no additional computational cost. These methods can be applied independently, each providing benefits, or together, with the potential for further performance improvements. Experimental results demonstrate the effectiveness of the proposed methods across various datasets. In particular, on K&K Logic Puzzle dataset, they enhance the performance of naive GRPO (trained from Qwen2.5-3B-Instruct) by 35.9% and 38.5%, respectively, and by 46.2% when used together.

In summary, our contributions are threefold: (1) We identify a critical issue in RL training for LLMs that has received limited attention: low-probability tokens disproportionately dominate the updates due to their large gradient contributions. (2) We provide a concise theoretical explanation for this phenomenon. (3) Based on the identified issue, we propose two simple yet effective methods, which significantly improve the downstream performance of GRPO-trained LLMs across various datasets.

2 Related Work

As a fundamental technique driving recent advancements in LLMs, reinforcement learning is attracting increasing attention from researchers. In this section, we provide a concise overview on the development of RL in the context of LLMs.

RL was pioneered by OpenAI as the final step of post-training to further align fine-tuned large models with human preferences [12, 13, 14, 15]. By leveraging vast amounts of human preference data and stable RL algorithms such as PPO [16], numerous enterprise-level language models have benefited from this approach and have been widely adopted. Notable examples include ChatGPT [17, 18], LLaMA [19, 20, 21], Qwen [22, 23, 24], Gemini [25, 26], and Claude [27]. Nevertheless, the challenges of collecting high-quality data that accurately reflect human preferences, the limited performance of open-source LLMs, and the computationally intensive training requirements of PPO-like online RL algorithms pose significant barriers for further exploring RL’s potentiality in the domain of LLMs. Most studies have focused on simplifying RL algorithms and directly leveraging preference data to optimize models. Representative works include Direct Preference Optimization (DPO) [28, 29], related analyses [30, 31, 32], and improved variants such as ORPO [33], CPO [34] and SimPO [35].

Recently, the emergence of long-chain-of-thought (CoT) [36] reasoning and its integration into both pre-training and post-training processes have significantly advanced the foundational capabilities of LLMs. OpenAI-o1 [1] was the first to demonstrate the remarkable potential of combining RL with CoT, enabling LLMs to surpass human cognitive abilities and tackle complex mathematical and coding tasks for the first time. Shortly thereafter, Deepseek-R1 [2] fully harnessed the potential of RL+CoT through a simple yet highly effective reinforcement learning algorithm GRPO [8]. Their findings revealed that LLMs exhibit human-like ‘aha moments’ during RL training. This achievement quickly garnered significant attention, inspiring extensive replication efforts [37, 38, 39, 40] stimulating further research on enhancing GRPO [9, 10] and PPO [41, 42], as well as comparative analyses between the two [11]. Nevertheless, most existing improvement solutions focus on enhancing sample quality, balancing response length, and preventing entropy collapse. To the best of our knowledge, this work is the first to improve RL training from the gradient-disproportionality perspective.

3 Preliminary

Large Language Models. Most existing LLMs are based on a transformer decoder-only architecture [43], typically denoted as π_θ , where $\theta \in \mathbb{R}^d$ represents the model parameters. The fundamental unit of LLMs is the token, a discrete textual element that may correspond to a word, subword, or character, and is drawn from a finite vocabulary $\mathcal{V} = \{v^1, \dots, v^N\}$, where N denotes the vocabulary size. During text generation, the model outputs a probability distribution over the vocabulary, conditioned on the given prompt \mathbf{q} and the sequence of previously generated tokens $\mathbf{o}_{<t}$. The next token o_t is then sampled from this distribution, expressed mathematically as $o_t \sim \pi_\theta(\cdot | \mathbf{q}, \mathbf{o}_{<t})$. The generation process is autoregressive, proceeding iteratively until either an end-of-sentence (EOS) token is produced or a predefined maximum sequence length t_{max} is reached. The resulting sequence of tokens is denoted as \mathbf{o} .

Practical LLMs are often required to align with human preferences or exhibit strong reasoning capabilities, which cannot be easily achieved through naive pre-training and supervised fine-tuning. If a reward function $r(\mathbf{q}, \mathbf{o})$ is available to quantitatively capture these objectives, the optimization of an LLM can be formulated as a reinforcement learning task. In this framework, the generation of each token is treated as an action, while the prompt and the previously generated tokens are treated as the state. Accordingly, the optimization objective of the LLM is expressed as $\max_\theta \mathbb{E}_{\mathbf{q} \sim \mathcal{D}, \mathbf{o} \sim \pi_\theta} [r(\mathbf{q}, \mathbf{o})]$, where \mathcal{D} is pre-collected dataset.

Group Relative Policy Optimization. As a widely used algorithm in early-stage research, PPO [16] requires a value model with as many—or even more—parameters as the model being trained. The value model must be trained in conjunction with LLMs, and its initialization adds complexity and uncertainties to the RL training process. To address these challenges, DeepSeek introduces GRPO [10], which eliminates the need for a value model entirely by estimating value through group-relative comparison. Specifically, for each question q , GRPO samples a group of outputs $\{\mathbf{o}_1, \mathbf{o}_2, \dots, \mathbf{o}_G\}$ and estimate the expected return under the question through $V(q) = \text{mean}(r(q, \mathbf{o}_1), r(q, \mathbf{o}_2), \dots)$. During the training process, the estimated advantage is set to be consistence within each responses ($\hat{A}_{i,t} = \hat{A}_i$), and is calculated through $\hat{A}_i = \frac{r(q, \mathbf{o}_i) - V(q)}{\text{std}(r(q, \mathbf{o}_1), r(q, \mathbf{o}_2), \dots)}$. Compared to PPO, GRPO reduces GPU memory overhead by 50% and decreases single-step RL training time by over 60% [38]. In this work, we adopt a variant of GRPO to optimize the policy model π_θ . The optimization objective is expressed as follows:

$$J_{GRPO}(\theta) = \mathbb{E}_{\mathbf{q} \sim \mathcal{D}, \{\mathbf{o}_i\}_{i=1}^G \sim \pi_{old}} \frac{1}{\sum_{i=1}^G |\mathbf{o}_i|} \sum_{i=1}^G \sum_{t=1}^{|\mathbf{o}_i|} \left\{ \min \left[r_{i,t}(\theta) \hat{A}_{i,t}, \text{clip}(r_{i,t}(\theta); 1 - \epsilon_l, 1 + \epsilon_h) \hat{A}_{i,t} \right] - \beta \mathbb{D}_{\text{KL}}[\pi_\theta \| \pi_{ref}] \right\}$$

with $r_{i,t}(\theta) = \frac{\pi_\theta(o_{i,t} | \mathbf{q}, \mathbf{o}_{i,<t})}{\pi_{old}(o_{i,t} | \mathbf{q}, \mathbf{o}_{i,<t})}$, and $\mathbb{D}_{\text{KL}}[\pi_\theta \| \pi_{ref}] = \frac{\pi_{ref}(o_{i,t} | \mathbf{q}, \mathbf{o}_{i,<t})}{\pi_\theta(o_{i,t} | \mathbf{q}, \mathbf{o}_{i,<t})} - \log \frac{\pi_{ref}(o_{i,t} | \mathbf{q}, \mathbf{o}_{i,<t})}{\pi_\theta(o_{i,t} | \mathbf{q}, \mathbf{o}_{i,<t})} - 1$, (1)

where π_{old} denotes the policy used to sample the responses, π_{ref} represents the initial policy prior to RL training, and $\epsilon_l, \epsilon_h, \beta$ are manually defined hyperparameters. Note that the original implementation of GRPO normalizes the token update weights based on the response length, which introduces a significant bias toward shorter responses during updates. In line with verl [44] and most follow-up work [40, 10], we remove this operation and conduct normalization among all tokens within the same query-batch.

4 Methodology

4.1 Explanation on Low-Probability Tokens' Dominance

In this section, we provide a theoretical explanation for why tokens with lower probabilities tend to dominate updates during RL training. The learning objective in Eq. (1) can be interpreted as a weighted cross-entropy loss. For simplicity, we use the notation $\pi(o_{i,t})$ to denote $\pi(o_{i,t} | \mathbf{q}, \mathbf{o}_{i,<t})$. By evaluating the gradient, we obtain the following expression (cf. Appendix A.1 for derivation):

$$\nabla_\theta J_{GRPO}(\theta) = \mathbb{E}_{\mathbf{q} \sim \mathcal{D}, \{\mathbf{o}_i\}_{i=1}^G \sim \pi_{old}} \frac{1}{\sum_{i=1}^G |\mathbf{o}_i|} \sum_{i=1}^G \sum_{t=1}^{|\mathbf{o}_i|} \underbrace{\left[\frac{\pi_\theta(o_{i,t})}{\pi_{old}(o_{i,t})} \hat{A}_{i,t} \cdot \mathbb{I}_{\text{trust}} \left(\frac{\pi_\theta(o_{i,t})}{\pi_{old}(o_{i,t})}, \hat{A}_{i,t} \right) + \beta \frac{\pi_{ref}(o_{i,t})}{\pi_\theta(o_{i,t})} - \beta \right]}_{w_{i,t}} \cdot \nabla_\theta \log \pi_\theta(o_{i,t}),$$

where $\mathbb{I}_{\text{trust}} \left(\frac{\pi_\theta(o_{i,t})}{\pi_{old}(o_{i,t})}, \hat{A}_{i,t} \right) = \begin{cases} 0 & \begin{cases} \text{if } \hat{A}_{i,t} > 0 \text{ and } \frac{\pi_\theta(o_{i,t})}{\pi_{old}(o_{i,t})} > 1 + \epsilon_h \\ \text{if } \hat{A}_{i,t} < 0 \text{ and } \frac{\pi_\theta(o_{i,t})}{\pi_{old}(o_{i,t})} < 1 - \epsilon_l \end{cases} \\ 1 & \text{otherwise} \end{cases}$.

We represent LLM as a composite function $f = f_L \circ f_{L-1} \circ \dots \circ f_1$, where each f_ℓ (with $\ell \in \{1, \dots, L\}$) corresponds to a distinct layer of the network. Let $a_{\ell-1}$ denote the input and a_ℓ denotes the output of ℓ th layer. We further define the Jacobian matrix of the ℓ th layer with respect to its input as $J_\ell := \frac{\partial f_\ell(a_{\ell-1})}{\partial a_{\ell-1}}$.

Assumption 4.1. *For every layer, the Jacobian J_ℓ is well-defined and the f_ℓ is locally differentiable. Furthermore, assume that for each layer, there exist two constants $c_\ell > 0$ and $d_\ell > 0$ such that $\sigma_{\min}(J_\ell) \geq c_\ell$ and $\sigma_{\max}(J_\ell) \leq d_\ell$, where $\sigma_{\min}(\cdot)$ and $\sigma_{\max}(\cdot)$ denote the minimum and maximum singular values of the given matrix, respectively.*

Assumption 4.1 is not restrictive, as it aligns with the standard design and training principles of neural-networks, ensuring stable gradients flow through well-defined and non-degenerate Jacobians.

Proposition 4.2. Under Assumption 4.1, let $\delta_\ell(o_{i,t}) := \nabla_{a_\ell} J_{GRPO}(o_{i,t})$ denote the gradient of the GRPO objective with respect to activation a_ℓ at any layer for a single token $o_{i,t}$. Let $\|\cdot\|$ denote the spectral norm, and define the vocabulary size as N . Then, for each layer ℓ , the following inequalities always hold:

$$\prod_{j=\ell+1}^L c_j \cdot |w_{i,t}| \cdot \sqrt{\frac{N}{N-1}} \cdot (1 - \pi_\theta(o_{i,t})) \leq \|\delta_\ell(o_{i,t})\| \leq \prod_{j=\ell+1}^L d_j \cdot |w_{i,t}| \cdot \sqrt{2} \cdot (1 - \pi_\theta(o_{i,t})). \quad (3)$$

Refer to Appendix A.2 for the detailed proof. Proposition 4.2 demonstrate that, for a single token, the gradient norm with respect to activation a_ℓ at any layer is bounded. Specifically, it is confined within the truncated conical region illustrated in Figure 2. In Eq. (3), apart from the term $(1 - \pi_\theta(o_{i,t}))$, all other components in these bounds can be regarded as constant. (Although $w_{i,t}$ depends on $\pi_\theta(o_{i,t})$, it is approximately equal to $\hat{A}_{i,t}$ in most cases.) This result highlights that *tokens with lower probabilities lead to larger gradient magnitudes, whereas tokens with probabilities approaching 1 produce gradients that are nearly zero*. The experimental evidence presented in Figure 1 corroborates this relationship, demonstrating a roughly proportional correspondence between the gradient norm of all LLM parameters and $(1 - \pi_\theta(o_{i,t}))$.

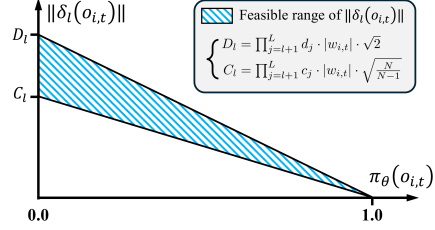


Figure 2: Diagram of Proposition 4.2.

Notably, during the RL training process, the gradients are averaged over hundreds of thousands of tokens for each update. Typically, the gradients are not sparsely distributed, leading to mutual influence among them. In such cases, low-probability tokens tend to dominate the gradient updates. Nevertheless, the gradients of high-probability tokens are equally important and should not be neglected (see Section 5.3 for details). To the best of our knowledge, no prior study has explicitly investigated the gradient interference between low-probability and high-probability tokens.

4.2 Mitigating the Over-Dominance of Low-Probability Tokens

Adverse Effect of the Dominance. A natural question arises: what are the consequences if the gradient of low-probability tokens over-dominates the update process? Experimental results in [11] suggest that positive samples (i.e., responses/tokens with an advantage greater than 0) play a more significant role than those negative ones. Theoretically, the probability of tokens with positive advantage should increase after each update. Thus, we record the proportion of positive tokens with increased probabilities during a single RL training step, as shown in Figure 3. In line with expectations, as the probability of a token grows, the proportion of updates in the correct direction decreases. In particular, the proportion of correct update directions for tokens with probability greater than 0.75 is even slightly less than 50%. To mitigate the over-dominance of low-probability tokens and promote more efficient updates for high-probability tokens, we introduce the following two methods.

Advantage Reweighting. A straightforward approach to address this issue is to reweight the advantage of tokens based on their probabilities. Specifically, we re-calculate the advantage of each token as follows:

$$\hat{A}_{i,t} = [\alpha \cdot \pi_\theta(o_{i,t}) + (1 - \alpha)] \cdot \hat{A}_{i,t}^{old}, \quad (4)$$

where $\alpha \in [0, 1]$ is a manually-defined hyperparameter. This formulation assigns linearly smaller update weights to tokens with lower probabilities. As shown in the upper panel of Figure 3, it can significantly reduce the errors in update directions for positive high-probability tokens.

Low-Probability Tokens Isolation (Lopti). In addition to *Advantage Reweighting*, we also explored an alternative method, referred to as *Lopti*. Specifically, for a sampled mini-batch in RL,

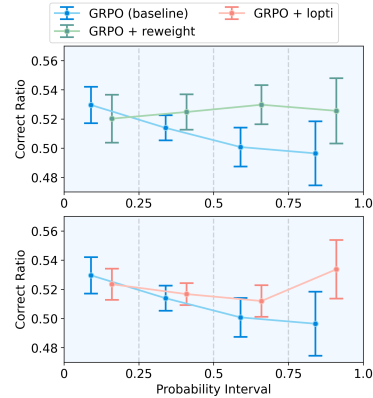


Figure 3: The proportion of positive tokens updated in the correct direction for different updating methods, under the same experimental settings as in Figure 1.

Algorithm 1 GRPO with Advantage Reweighting and Low-Probability Token Isolation

Require: Initial LLM $\pi_\theta = \pi_{ref}$, datasets $\mathcal{D} = \{q\}$, reward function $r(q, o)$, reweighting hyperparameter α , isolation threshold η

```
1: for each dataset epoch do
2:   for each RL step, sample  $\{q\}^M \sim \mathcal{D}$  do
3:     Auto-regress sampling  $G$  responses  $\{o_i\}_{i=1}^G$  for each question within  $\{q\}^M$ 
4:     Record the old probability for each token  $\pi_{old}(o_{i,t}) = \pi_\theta(o_{i,t})$ 
5:     Calculate the reward for each response with reward function  $r(q, o_i)$ 
6:     Calculate the advantage for each token (response) through  $\hat{A}_{i,t} = \hat{A}_i = \frac{r(q, o_i) - \text{mean}\{r(q, o_i)\}_{i=1}^G}{\text{std}\{r(q, o_i)\}_{i=1}^G}$ 
7:     Reweight Advantage through Eq. (4)
8:     for each RL epoch, sample mini_batch  $\sim \{q, \{\{\hat{A}_{i,t}, \pi_{old}(o_{i,t})\}_{t=1}^{|o_i|}\}_{i=1}^G\}^M$  do
9:       Update the policy  $\pi_\theta$  with mini_batch through Eq. (1)
10:    end for
11:    Record the old Advantage  $\hat{A}_{i,t}^{old} = \hat{A}_{i,t}$ 
12:    Mask high-probability tokens through  $\hat{A}_{i,t} = \hat{A}_{i,t}^{old} \odot \mathbb{I}(\pi_{old}(o_{i,t}) \leq \eta)$ 
13:    for each RL epoch, sample mini_batch  $\sim \{q, \{\{\hat{A}_{i,t}, \pi_{old}(o_{i,t})\}_{t=1}^{|o_i|}\}_{i=1}^G\}^M$  do
14:      Update the policy  $\pi_\theta$  with mini batch through Eq. (1)
15:    end for
16:    Mask low-probability tokens  $\hat{A}_{i,t} = \hat{A}_{i,t}^{old} \odot (1 - \mathbb{I}(\pi_{old}(o_{i,t}) \leq \eta))$ 
17:    for each RL epoch, sample mini_batch  $\sim \{q, \{\{\hat{A}_{i,t}, \pi_{old}(o_{i,t})\}_{t=1}^{|o_i|}\}_{i=1}^G\}^M$  do
18:      Update the policy  $\pi_\theta$  with mini batch through Eq. (1)
19:    end for
20:  end for
21: end for
22: return Final policy  $\pi_\theta$ 
```

we predefine a probability threshold $\eta \in (0, 1)$ to divide tokens into two groups: low-probability tokens and high-probability tokens. We first update the low-probability tokens, followed by the high-probability tokens. For detailed implementation, please refer to lines 11–19 of Algorithm 1. With a universal hyperparameter setting of $\eta = 0.5$, this method achieves a comparable effect to *Advantage Reweighting*, as shown in the lower panel of Figure 3.

The intuition behind *Lopti* is as follows: during the first stage, updates on low-probability tokens indirectly influence the distribution of the remaining high-probability tokens that have not yet been updated (as in Figure 1(e)). If a positive high-probability token is affected in the correct direction (i.e., its probability increases), its gradient becomes smaller in the subsequent stage when high-probability tokens are updated. Conversely, if its probability decreases, its gradient will dominate within the high-probability token group, thereby receiving greater attention during the update process. Note that the order of updates cannot be reversed. The corresponding ablation is presented in Section 5.3.

It is worth noting that *Advantage Reweighting* and *Lopti* can operate concurrently and may even lead to further improved downstream performance. In Algorithm 1, we detail how to integrate these two techniques with GRPO. Note that the original GRPO update step (the gray section with strikethrough in lines 8–10) should be skipped if *Lopti* is activated. The computational cost requirements are detailed in Appendix C.2. Since *Lopti* splits the tokens and performs updates twice, it results in higher computational costs, which is a limitation of our method (cf. Appendix E).

5 Experimental Results

To validate the effectiveness of our proposed method, we first conduct experiments on the Knights and Knaves (K&K) Logic Puzzles dataset [38, 45] using GRPO, as described in Section 5.1. We then extend the experiments to the math-related dataset [37, 42], as detailed in Section 5.2. Finally, we present a series of critical ablation studies, as outlined in Section 5.3. Note that our methods are not restricted to GRPO and hold great potential across all Policy-Gradient based RL algorithms. For experiments utilizing REINFORCE++ [46], please refer to Appendix D.

5.1 Experiments on K&K Logic Puzzles

The K&K logic puzzles, first aggregated into a benchmark for LLMs by Xie et al. [45], are a class of reasoning problems rooted in classical logic game [47, 48]. These puzzles involve a fictional scenario

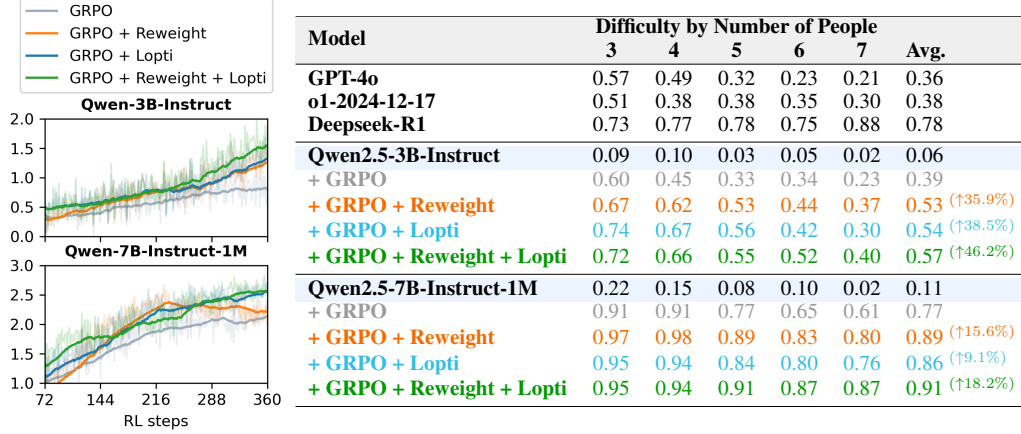


Figure 4: Experimental results on the K&K Logic Puzzles benchmark. For *Advantage Reweight*, $\alpha = 0.3$, and for *Lopti*, $\eta = 0.5$. The reward curve during training (left) is truncated to exclude the first epoch and smoothed with an exponential moving average (coefficient: 0.95). The evaluation accuracy on the test set (right) are averaged over the last three checkpoints to mitigate randomness.

where inhabitants of an island are either Knights, who always tell the truth, or Knaves, who always lie. The objective is to determine the identity of each inhabitant (Knight or Knave) based on a set of statements they make about themselves and others. Please refer to Appendix C.1.1 for detailed introduction. The K&K logic puzzles are highly challenging, with only the most advanced LLMs demonstrating strong performance [45]. Additionally, it is not exposed in the model’s pre-training phase, allowing the model to demonstrate continual learning behavior during training. As training progresses, both the training reward and test accuracy gradually improve, rather than converging rapidly. These characteristics make this benchmark an ideal choice for verifying RL performance.

Following Logic-RL [38], we construct the training set by combining logic puzzles with 3 to 7 players and adopt its rule-based reward function, which consists of two components: (1) Format score, assigned 1 if the model provides CoT reasoning within `<think></think>` tags and the final answer within `<answer></answer>` tags, and -1 otherwise; (2) Answer reward, assigned 2 for a perfect match with the ground truth, -1.5 for partial correctness, and -2 for an completely incorrect answer. We use Qwen2.5-3B-Instruct and Qwen2.5-7B-Instruct-1M as starting points. Without employing curriculum learning, we directly expose the model to the mixed training set and train it for a total of

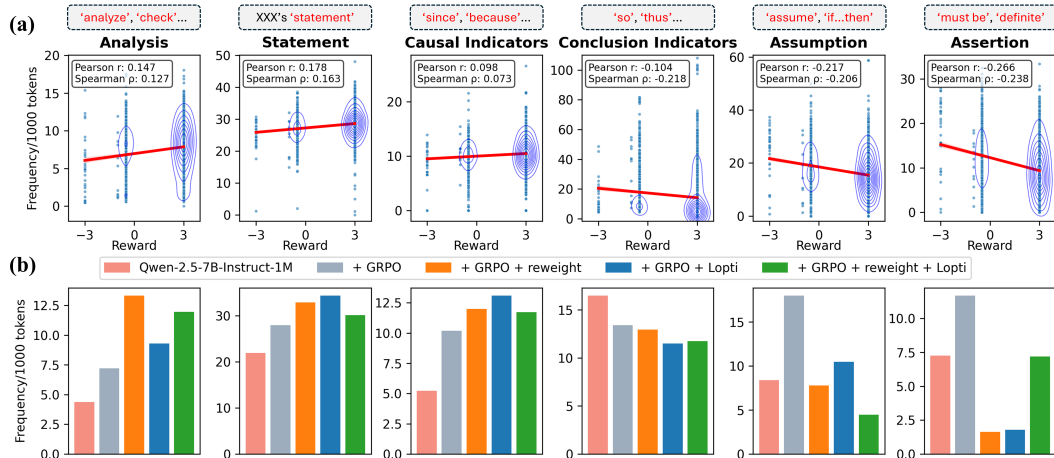


Figure 5: (a) The relationship between the frequency of six categories of inference-related words and the corresponding sample rewards for Qwen-2.5-7B-Instruct-1M trained with naive GRPO. The Pearson correlation coefficient (r) and Spearman rank correlation coefficient (ρ) are annotated. (b) A comparison of the frequency of the six categories of words across the starting point (Qwen-2.5-7B-Instruct-1M), naive GRPO, and GRPO enhanced with Advantage Reweighting and/or Lopti.

Table 1: Experimental results on math-related datasets (DSR for DeepScaleR and ORZ for Open-Reasoner-Zero). For *Advantage Reweight*, α is set to 0.1, and for *Lopti*, η is set to 0.5. The evaluation accuracy(%) are averaged over the last three checkpoints to mitigate randomness.

Dataset	Algorithms	Olympiad Bench	Minerva	MATH 500	AMC avg@16	AIME24 pass@16	AIME24 avg@16	Avg. all
Qwen2.5-7B		27.64	18.38	63.00	22.21	30.00	5.00	27.71
DSR Uniform	+ GRPO	36.50	29.66	74.67	47.72	28.89	16.46	38.98
	+ GRPO + Reweight	37.00	29.66	75.47	48.32	35.56	14.03	40.01
	+ GRPO + Lopti	36.60	30.27	76.53	47.69	32.22	14.24	39.59
ORZ	+ GRPO	38.23	27.69	78.33	49.57	32.22	12.92	39.83
	+ GRPO + Reweight	40.81	29.04	77.80	49.07	33.33	16.46	41.09
	+ GRPO + Lopti	38.63	29.78	78.53	47.29	34.44	15.28	40.66

5 epochs. The experimental results are reported in Figure 4. Detailed hyperparameter settings are provided in Appendix B, and comprehensive experimental records can be found in Appendix C.1.1.

During the early stages of GRPO training (across all settings), the reward increases rapidly, but the growth slows significantly after the first epoch. Subsequently, the improvements introduced by *Advantage Reweighting* and *Lopti* become progressively more evident, particularly after 4 epochs. Interestingly, for simpler tasks (involving fewer players), the performance gap between the baseline GRPO and the GRPO enhanced with *Advantage Reweighting* and/or *Lopti* is minimal. However, for more complex tasks with more players, the performance gap becomes significant. In challenging tasks, positive samples are typically fewer and thus more valuable. As analyzed in Section 4.2, high-probability tokens in these rare positive samples are not effectively amplified under standard GRPO training. Our method addresses this limitation, thereby resulting in substantial performance improvements.

In addition, we perform a linguistic analysis to investigate the correlation between the model’s reasoning behavior and its final performance. Specifically, we use the model trained with naive GRPO to generate responses for the 500 prompts in the test set, sampling 8 responses per prompt, resulting in a total of 4,000 samples. For these samples, we analyze the frequency of six categories of inference-related words (see Appendix C.1.1 for details) and their corresponding rule-based rewards, as illustrated in Figure 5(a). The analysis reveals a positive correlation between the frequency of words in the categories *Analysis*, *Statement*, and *Causal Indicators* and the samples’ rewards. Conversely, the frequency of words in the categories *Conclusion Indicator*, *Assumption*, and *Assertion* exhibits a negative correlation with the rewards.

It is worth noting that the statistical patterns observed in these six categories of words indirectly highlight the enhancement effects of our proposed *Advantage Reweighting* and/or *Lopti* mechanisms on GRPO training, as shown in Figure 5(b). Notably, the frequency of words positively correlated with reward in the samples generated by our method is significantly higher than that of the baseline, while the frequency of words negatively correlated with reward is substantially lower.

5.2 Experiments on Math-related Datasets

To assess the generalization capability of our proposed methods, we conduct additional experiments on math-related datasets. Consistent with the majority of prior studies, we utilize Qwen2.5-7B as the base model and employ a straightforward rule-based reward. Specifically, a score of 1 is assigned for completely correct answers, while a score of 0 is given for all other cases. We experiment with two different datasets. The first one is a subset containing 10k problems introduced by AdaRFT [42], which is sampled from DeepScaleR [37]. This dataset, referred to as DSR-Uniform, evenly covers problems across all difficulty levels and is specifically designed for Qwen2.5-7B. We train this dataset for 5 epochs. The second one is a dataset containing 57k problems introduced by Open-Reasoner-Zero (ORZ) [10]. For this dataset (ORZ), we train for 1 epoch. Apart from the number of training epochs, all other hyperparameters (cf. Appendix B) are kept consistent across both datasets.

We evaluate the LLMs after training on five benchmarks: Olympiad Bench [49], Minerva [50], MATH-500 [51], AMC 2022-2023, and AIME 2024. For the first three benchmarks, we use greedy sampling for evaluation. For the last two benchmarks, following most prior works, we sample 16 responses for each question and report the average accuracy (avg@16). Notably, AIME 2024 is

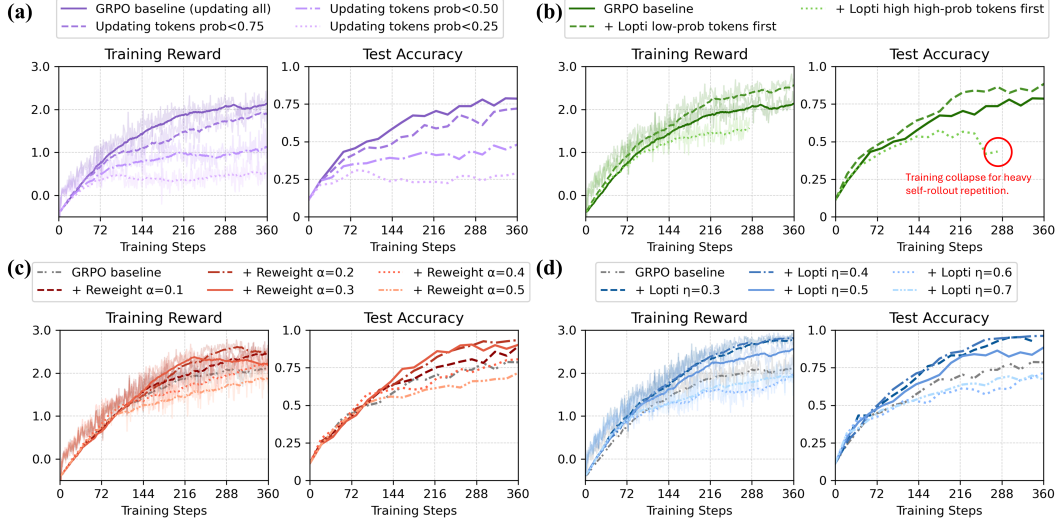


Figure 6: Ablation studies on the K&K Logic Puzzles dataset. (a) Effect of restricting updates to high-probability tokens. (b) Effect of the token update order in *Lopti*. (c) Effect of the hyperparameter α in *Advantage Reweighting*. (d) Effect of the hyperparameter η in *Lopti*.

an extremely challenging dataset; therefore, we also report pass@16, which considers a question correctly answered if at least one of the 16 responses is correct.

The experimental results are summarized in Table 1. In contrast to the continual learning behavior observed in the K&K Logic Puzzle dataset, the test accuracy curve on the math-related dataset converges to a specific value within 100 steps and subsequently exhibits only minor fluctuations. Despite this, the improvements introduced by our *Advantage Reweighting* and *Lopti* remain observable. It is worth noting that the combined application of these two techniques does not result in further performance gains; therefore, we recommend using them individually for optimal results. For detailed experimental records, please refer to Appendix C.1.2.

5.3 Ablation Studies

To better convey our motivation and demonstrate the effectiveness of the proposed methods, we perform ablation studies on the K&K Logic Puzzles dataset. The key conclusions derived from these studies are summarized in the following three points.

- **High-probability tokens matter in RL training.** Although the results in Figure 1 and Figure 3 suggest that the gradients of high-probability tokens are almost suppressed by low-probability tokens during updates, the high-probability tokens remain crucial and cannot be disregarded. As shown in Figure 6(a), masking high-probability tokens leads to a significant degradation in the performance of the baseline GRPO. Therefore, reducing the influence of low-probability tokens on high-probability ones holds great potential for advancing RL training, as anticipated.

- **The update order is the key for *Lopti*.** The intuition behind *Lopti*, as introduced in Section 4.2, stems from the *low-probability dominant effect* of incorrectly reduced positive high-probability tokens. To confirm this intuition and rule out the possibility of random gains, we reverse the update order by processing high-probability tokens first, followed by low-probability tokens, as shown in Figure 6(b). This modification leads to significantly worse performance compared to the GRPO baseline, with training even collapsing after the 4th epoch.

- **Proper hyperparameter tuning is essential for *Advantage Reweighting* and *Lopti*.** As introduced in Section 4.2, *Advantage Reweighting* involves the hyperparameter α , while *Lopti* depends on the hyperparameter η . For the K&K Logic Puzzles dataset, the recommended ranges are $\alpha \in [0.2, 0.3]$ and $\eta \in [0.3, 0.5]$, as values outside these ranges may result in inferior performance compared to the GRPO baseline. It is worth noting that the hyperparameter setting for *Advantage Reweighting* is task-sensitive, whereas *Lopti* demonstrates greater robustness in this regard. For math-related datasets, the optimal hyperparameter for *Advantage Reweighting* is $\alpha = 0.1$, while *Lopti* maintains its robustness with $\eta = 0.5$.

6 Conclusion

In this paper, we identify a crucial issue in RL training for LLMs: the over-dominance of low-probability tokens in model updates due to their disproportionately large gradient magnitudes. We substantiate this issue through both empirical observations and rigorous theoretical analysis. To address this imbalance, we propose two novel approaches: *Advantage Reweighting* and *Lopti*. These methods effectively mitigate gradient disparities by diminishing the undue influence of low-probability tokens, thereby facilitating more balanced and efficient updates for high-probability tokens. Extensive experiments demonstrate the effectiveness of these approaches, showing consistent improvements in GRPO-trained LLMs across diverse base models and datasets.

References

- [1] Aaron Jaech, Adam Kalai, Adam Lerer, Adam Richardson, Ahmed El-Kishky, Aiden Low, Alec Helyar, Aleksander Madry, Alex Beutel, Alex Carney, et al. OpenAI o1 system card. [arXiv preprint arXiv:2412.16720](#), 2024.
- [2] Daya Guo, Dejian Yang, Haowei Zhang, Junxiao Song, Ruoyu Zhang, Runxin Xu, Qihao Zhu, Shiron Ma, Peiyi Wang, Xiao Bi, et al. Deepseek-R1: Incentivizing reasoning capability in LLMs via reinforcement learning. [arXiv preprint arXiv:2501.12948](#), 2025.
- [3] Kimi Team, Angang Du, Bofei Gao, Bowei Xing, Changjiu Jiang, Cheng Chen, Cheng Li, Chenjun Xiao, Chenzhuang Du, Chonghua Liao, et al. Kimi k1.5: Scaling reinforcement learning with LLMs. [arXiv preprint arXiv:2501.12599](#), 2025.
- [4] Yuxi Xie, Anirudh Goyal, Wenye Zheng, Min-Yen Kan, Timothy P Lillicrap, Kenji Kawaguchi, and Michael Shieh. Monte carlo tree search boosts reasoning via iterative preference learning. [The First Workshop on System-2 Reasoning at Scale, NeurIPS’24](#), 2024.
- [5] Guoxin Chen, Minpeng Liao, Chengxi Li, and Kai Fan. Alphamath almost zero: Process supervision without process. In [Advances in Neural Information Processing Systems](#), volume 38, 2024.
- [6] Hunter Lightman, Vineet Kosaraju, Yuri Burda, Harrison Edwards, Bowen Baker, Teddy Lee, Jan Leike, John Schulman, Ilya Sutskever, and Karl Cobbe. Let’s verify step by step. In [The Twelfth International Conference on Learning Representations](#), 2024.
- [7] Peiyi Wang, Lei Li, Zhihong Shao, Runxin Xu, Damai Dai, Yifei Li, Deli Chen, Yu Wu, and Zhifang Sui. Math-shepherd: Verify and reinforce llms step-by-step without human annotations. In [Proceedings of the 62nd Annual Meeting of the Association for Computational Linguistics](#), 2024.
- [8] Zhihong Shao, Peiyi Wang, Qihao Zhu, Runxin Xu, Junxiao Song, Xiao Bi, Haowei Zhang, Mingchuan Zhang, YK Li, Y Wu, et al. Deepseekmath: Pushing the limits of mathematical reasoning in open language models. [arXiv preprint arXiv:2402.03300](#), 2024.
- [9] Qiyang Yu, Zheng Zhang, Ruofei Zhu, Yufeng Yuan, Xiaochen Zuo, Yu Yue, Tiantian Fan, Gaohong Liu, Lingjun Liu, Xin Liu, et al. DAPO: An open-source llm reinforcement learning system at scale. [arXiv preprint arXiv:2503.14476](#), 2025.
- [10] Zichen Liu, Changyu Chen, Wenjun Li, Penghui Qi, Tianyu Pang, Chao Du, Wee Sun Lee, and Min Lin. Understanding rl-zero-like training: A critical perspective. [arXiv preprint arXiv:2503.20783](#), 2025.
- [11] Wei Xiong, Jiarui Yao, Yuhui Xu, Bo Pang, Lei Wang, Doyen Sahoo, Junnan Li, Nan Jiang, Tong Zhang, Caiming Xiong, et al. A minimalist approach to llm reasoning: from rejection sampling to reinforce. [arXiv preprint arXiv:2504.11343](#), 2025.
- [12] Paul F Christiano, Jan Leike, Tom Brown, Miljan Martic, Shane Legg, and Dario Amodei. Deep reinforcement learning from human preferences. In [Advances in Neural Information Processing Systems](#), volume 31, 2017.

- [13] Daniel M Ziegler, Nisan Stiennon, Jeffrey Wu, Tom B Brown, Alec Radford, Dario Amodei, Paul Christiano, and Geoffrey Irving. Fine-tuning language models from human preferences. arXiv preprint arXiv:1909.08593, 2019.
- [14] Nisan Stiennon, Long Ouyang, Jeffrey Wu, Daniel Ziegler, Ryan Lowe, Chelsea Voss, Alec Radford, Dario Amodei, and Paul F Christiano. Learning to summarize with human feedback. In Advances in Neural Information Processing Systems, volume 34, 2020.
- [15] Long Ouyang, Jeffrey Wu, Xu Jiang, Diogo Almeida, Carroll Wainwright, Pamela Mishkin, Chong Zhang, Sandhini Agarwal, Katarina Slama, Alex Ray, et al. Training language models to follow instructions with human feedback. In Advances in Neural Information Processing Systems, volume 36, 2022.
- [16] John Schulman, Filip Wolski, Prafulla Dhariwal, Alec Radford, and Oleg Klimov. Proximal policy optimization algorithms. arXiv preprint arXiv:1707.06347, 2017.
- [17] Tom Brown, Benjamin Mann, Nick Ryder, Melanie Subbiah, Jared D Kaplan, Prafulla Dhariwal, Arvind Neelakantan, Pranav Shyam, Girish Sastry, Amanda Askell, et al. Language models are few-shot learners. In Advances in Neural Information Processing Systems, volume 34, 2020.
- [18] Josh Achiam, Steven Adler, Sandhini Agarwal, Lama Ahmad, Ilge Akkaya, Florencia Leoni Aleman, Diogo Almeida, Janko Altschmidt, Sam Altman, Shyamal Anadkat, et al. GPT-4 technical report. arXiv preprint arXiv:2303.08774, 2023.
- [19] Hugo Touvron, Thibaut Lavril, Gautier Izacard, Xavier Martinet, Marie-Anne Lachaux, Timothée Lacroix, Baptiste Rozière, Naman Goyal, Eric Hambro, Faisal Azhar, et al. LLaMA: Open and efficient foundation language models. arXiv preprint arXiv:2302.13971, 2023.
- [20] Hugo Touvron, Louis Martin, Kevin Stone, Peter Albert, Amjad Almahairi, Yasmine Babaei, Nikolay Bashlykov, Soumya Batra, Prajwal Bhargava, Shruti Bhosale, et al. LLaMA 2: Open foundation and fine-tuned chat models. arXiv preprint arXiv:2307.09288, 2023.
- [21] Abhimanyu Dubey, Abhinav Jauhri, Abhinav Pandey, Abhishek Kadian, Ahmad Al-Dahle, Aiesha Letman, Akhil Mathur, Alan Schelten, Amy Yang, Angela Fan, et al. The LLaMA 3 herd of models. arXiv preprint arXiv:2407.21783, 2024.
- [22] Jinze Bai, Shuai Bai, Yunfei Chu, Zeyu Cui, Kai Dang, Xiaodong Deng, Yang Fan, Wenbin Ge, Yu Han, Fei Huang, et al. Qwen technical report. arXiv preprint arXiv:2309.16609, 2023.
- [23] Yunfei Chu, Jin Xu, Xiaohuan Zhou, Qian Yang, Shiliang Zhang, Zhijie Yan, Chang Zhou, and Jingren Zhou. Qwen-audio: Advancing universal audio understanding via unified large-scale audio-language models. arXiv preprint arXiv:2311.07919, 2023.
- [24] An Yang, Baosong Yang, Binyuan Hui, Bo Zheng, Bowen Yu, Chang Zhou, Chengpeng Li, Chengyuan Li, Dayiheng Liu, Fei Huang, et al. Qwen2 technical report. arXiv preprint arXiv:2407.10671, 2024.
- [25] Gemini Team, Rohan Anil, Sebastian Borgeaud, Jean-Baptiste Alayrac, Jiahui Yu, Radu Soricut, Johan Schalkwyk, Andrew M Dai, Anja Hauth, Katie Millican, et al. Gemini: a family of highly capable multimodal models. arXiv preprint arXiv:2312.11805, 2023.
- [26] Gemini Team, Petko Georgiev, Ving Ian Lei, Ryan Burnell, Libin Bai, Anmol Gulati, Garrett Tanzer, Damien Vincent, Zhufeng Pan, Shibo Wang, et al. Gemini 1.5: Unlocking multimodal understanding across millions of tokens of context. arXiv preprint arXiv:2403.05530, 2024.
- [27] Anthropic. The Claude 3 model family: Opus, sonnet, haiku. Technical Report, 2024.
- [28] Rafael Rafailov, Archit Sharma, Eric Mitchell, Christopher D Manning, Stefano Ermon, and Chelsea Finn. Direct preference optimization: Your language model is secretly a reward model. In Advances in Neural Information Processing Systems, volume 37, 2023.
- [29] Rafael Rafailov, Joey Hejna, Ryan Park, and Chelsea Finn. From r to Q*: Your language model is secretly a Q-function. In First Conference on Language Modeling, 2024.

- [30] Shusheng Xu, Wei Fu, Jiaxuan Gao, Wenjie Ye, Weilin Liu, Zhiyu Mei, Guangju Wang, Chao Yu, and Yi Wu. Is DPO superior to PPO for LLM alignment? a comprehensive study. In International Conference on Machine Learning, volume 41, 2024.
- [31] Han Zhong, Guhao Feng, Wei Xiong, Xinle Cheng, Li Zhao, Di He, Jiang Bian, and Liwei Wang. DPO meets PPO: Reinforced token optimization for RLHF. In ICML 2024 Workshop on Models of Human Feedback for AI Alignment, 2024.
- [32] Yi Ren and Danica J. Sutherland. Learning dynamics of LLM finetuning. In The Thirteenth International Conference on Learning Representations, 2025.
- [33] Jiwoo Hong, Noah Lee, and James Thorne. ORPO: Monolithic preference optimization without reference model. In Proceedings of the 2024 Conference on Empirical Methods in Natural Language Processing, 2024.
- [34] Haoran Xu, Amr Sharaf, Yunmo Chen, Weiting Tan, Lingfeng Shen, Benjamin Van Durme, Kenton Murray, and Young Jin Kim. Contrastive preference optimization: Pushing the boundaries of llm performance in machine translation. In International Conference on Machine Learning, volume 41, 2024.
- [35] Yu Meng, Mengzhou Xia, and Danqi Chen. SimPO: Simple preference optimization with a reference-free reward. In Advances in Neural Information Processing Systems, volume 38, 2024.
- [36] Jason Wei, Xuezhi Wang, Dale Schuurmans, Maarten Bosma, Fei Xia, Ed Chi, Quoc V Le, Denny Zhou, et al. Chain-of-thought prompting elicits reasoning in large language models. In Advances in Neural Information Processing Systems, volume 36, 2022.
- [37] Michael Luo, Sijun Tan, Justin Wong, Xiaoxiang Shi, William Y. Tang, Manan Roongta, Colin Cai, Jeffrey Luo, Li Erran Li, Raluca Ada Popa, and Ion Stoica. Deepscaler: Surpassing o1-preview with a 1.5b model by scaling rl. Notion Blog, 2025.
- [38] Tian Xie, Zitian Gao, Qingnan Ren, Haoming Luo, Yuqian Hong, Bryan Dai, Joey Zhou, Kai Qiu, Zhirong Wu, and Chong Luo. Logic-rl: Unleashing llm reasoning with rule-based reinforcement learning. arXiv preprint arXiv:2502.14768, 2025.
- [39] Jingcheng Hu, Yinmin Zhang, Qi Han, Daxin Jiang, Xiangyu Zhang, and Heung-Yeung Shum. Open-reasoner-zero: An open source approach to scaling up reinforcement learning on the base model. arXiv preprint arXiv:2503.24290, 2025.
- [40] Weihao Zeng, Yuzhen Huang, Qian Liu, Wei Liu, Keqing He, Zejun Ma, and Junxian He. Simplerl-zoo: Investigating and taming zero reinforcement learning for open base models in the wild. arXiv preprint arXiv:2503.18892, 2025.
- [41] Yufeng Yuan, Qiyang Yu, Xiaochen Zuo, Ruofei Zhu, Wenyuan Xu, Jiaze Chen, Chengyi Wang, TianTian Fan, Zhengyin Du, Xiangpeng Wei, et al. VAPO: Efficient and reliable reinforcement learning for advanced reasoning tasks. arXiv preprint arXiv:2504.05118, 2025.
- [42] Taiwei Shi, Yiyang Wu, Linxin Song, Tianyi Zhou, and Jieyu Zhao. Efficient reinforcement finetuning via adaptive curriculum learning. arXiv preprint arXiv:2504.05520, 2025.
- [43] Ashish Vaswani, Noam Shazeer, Niki Parmar, Jakob Uszkoreit, Llion Jones, Aidan N Gomez, Łukasz Kaiser, and Illia Polosukhin. Attention is all you need. In Advances in Neural Information Processing Systems, volume 30, 2017.
- [44] Guangming Sheng, Chi Zhang, Zilingfeng Ye, Xibin Wu, Wang Zhang, Ru Zhang, Yanghua Peng, Haibin Lin, and Chuan Wu. Hybridflow: A flexible and efficient RLHF framework. Proceedings of the Twentieth European Conference on Computer Systems, 2025.
- [45] Chulin Xie, Yangsibo Huang, Chiyuan Zhang, Da Yu, Xinyun Chen, Bill Yuchen Lin, Bo Li, Badih Ghazi, and Ravi Kumar. On memorization of large language models in logical reasoning. arXiv preprint arXiv:2410.23123, 2024.

- [46] Jian Hu. Reinforce++: A simple and efficient approach for aligning large language models. arXiv preprint arXiv:2501.03262, 2025.
- [47] Raymond Smullyan. What is the name of this book? Touchstone Books Guildford, UK, 1986.
- [48] Philip N Johnson-Laird and Ruth MJ Byrne. Meta-logical problems: Knights, knaves, and rips. Cognition, 36(1):69–84, 1990.
- [49] Chaoqun He, Renjie Luo, Yuzhuo Bai, Shengding Hu, Zhen Thai, Junhao Shen, Jinyi Hu, Xu Han, Yujie Huang, Yuxiang Zhang, et al. Olympiadbench: A challenging benchmark for promoting agi with olympiad-level bilingual multimodal scientific problems. Proceedings of the 62nd Annual Meeting of the Association for Computational Linguistics, 2024.
- [50] Aitor Lewkowycz, Anders Andreassen, David Dohan, Ethan Dyer, Henryk Michalewski, Vinay Ramasesh, Ambrose Slone, Cem Anil, Imanol Schlag, Theo Gutman-Solo, et al. Solving quantitative reasoning problems with language models. In Advances in Neural Information Processing Systems, volume 36, 2022.
- [51] Dan Hendrycks, Collin Burns, Saurav Kadavath, Akul Arora, Steven Basart, Eric Tang, Dawn Song, and Jacob Steinhardt. Measuring mathematical problem solving with the math dataset. arXiv preprint arXiv:2103.03874, 2021.
- [52] John Schulman. Approximating KL divergence. Technical Blog, 2020.
- [53] Ronald J Williams. Simple statistical gradient-following algorithms for connectionist reinforcement learning. Machine learning, 8:229–256, 1992.

A Theoretical Interpretations

A.1 Gradient Derivation for the GRPO Objective

For clarity, we re-state the objective function of GRPO below:

$$J_{GRPO}(\theta) = \mathbb{E}_{\mathbf{q} \sim \mathcal{D}, \{\mathbf{o}_i\}_{i=1}^G \sim \pi_{old}} \left\{ \frac{1}{\sum_{i=1}^G |\mathbf{o}_i|} \sum_{i=1}^G \sum_{t=1}^{|\mathbf{o}_i|} \left\{ \underbrace{\min \left[r_{i,t}(\theta) \hat{A}_i, \text{clip}(r_{i,t}(\theta); 1 - \epsilon_l, 1 + \epsilon_h) \hat{A}_i \right]}_{J_{policy}(\theta)} - \underbrace{\beta \mathbb{D}_{KL}[\pi_\theta \| \pi_{ref}]}_{J_{KL}(\theta)} \right\} \right\} \quad (5)$$

with $r_{i,t}(\theta) = \frac{\pi_\theta(o_{i,t})}{\pi_{old}(o_{i,t})}$, and $\mathbb{D}_{KL}[\pi_\theta \| \pi_{ref}] = \frac{\pi_{ref}(o_{i,t})}{\pi_\theta(o_{i,t})} - \log \frac{\pi_{ref}(o_{i,t})}{\pi_\theta(o_{i,t})} - 1$.

We begin by analyzing the policy loss term $J_{policy}(\theta)$, which originates from the PPO clipping mechanism [16]. Note that for samples with positive advantage estimates (i.e., $\hat{A}_i > 0$), the clipping is activated only when $r_{i,t}(\theta) > 1 + \epsilon_h$. Conversely, for samples with negative advantage estimates (i.e., $\hat{A}_i < 0$), the clipping becomes active only when $r_{i,t}(\theta) < 1 - \epsilon_l$. Consequently, when clipping is active, the gradient $\nabla_\theta J_{policy}(\theta)$ is zero; otherwise, it simplifies to $\nabla_\theta r_{i,t}(\theta) \cdot \hat{A}_i$. In summary, we can express the gradient of $J_{policy}(\theta)$ as

$$\begin{aligned} \nabla_\theta J_{policy}(\theta) &= \frac{\nabla_\theta \pi_\theta(o_{i,t})}{\pi_{old}(o_{i,t})} \cdot \hat{A}_i \cdot \mathbb{I}_{\text{trust}}\left(\frac{\pi_\theta(o_{i,t})}{\pi_{old}(o_{i,t})}, \hat{A}_i\right) \\ &= \frac{\pi_\theta(o_{i,t})}{\pi_{old}(o_{i,t})} \cdot \hat{A}_i \cdot \mathbb{I}_{\text{trust}}\left(\frac{\pi_\theta(o_{i,t})}{\pi_{old}(o_{i,t})}, \hat{A}_i\right) \nabla_\theta \log \pi_\theta(o_{i,t}) \end{aligned} \quad (6)$$

where $\mathbb{I}_{\text{trust}}\left(\frac{\pi_\theta(o_{i,t})}{\pi_{old}(o_{i,t})}, \hat{A}_i\right) = \begin{cases} 0 & \begin{cases} \text{if } \hat{A}_i > 0 \text{ and } \frac{\pi_\theta(o_{i,t})}{\pi_{old}(o_{i,t})} > 1 + \epsilon_h \\ \text{if } \hat{A}_i < 0 \text{ and } \frac{\pi_\theta(o_{i,t})}{\pi_{old}(o_{i,t})} < 1 - \epsilon_l \end{cases} \\ 1 & \text{otherwise} \end{cases}$.

Next, we consider the KL constraint term $J_{KL}(\theta)$, commonly referred to as k_3 estimation [52]. It provides an unbiased estimate of the KL divergence between the current policy and the reference policy. The gradient of $J_{KL}(\theta)$ is given by:

$$\begin{aligned} \nabla_\theta J_{KL}(\theta) &= \beta \nabla_\theta \frac{\pi_{ref}(o_{i,t})}{\pi_\theta(o_{i,t})} + \beta \nabla_\theta \log \pi_\theta(o_{i,t}) \\ &= -\beta \frac{\pi_{ref}(o_{i,t})}{\pi_\theta(o_{i,t})^2} \nabla_\theta \pi_\theta(o_{i,t}) + \beta \nabla_\theta \log \pi_\theta(o_{i,t}) \\ &= -\left[\beta \frac{\pi_{ref}(o_{i,t})}{\pi_\theta(o_{i,t})} - \beta \right] \nabla_\theta \log \pi_\theta(o_{i,t}). \end{aligned} \quad (7)$$

By combining Eqs. (6) and (7), we finally obtain the gradient of GRPO objective in the following form.

$$\begin{aligned} \nabla_\theta J_{GRPO}(\theta) &= \mathbb{E}_{\mathbf{q} \sim \mathcal{D}, \{\mathbf{o}_i\}_{i=1}^G \sim \pi_{old}} \frac{1}{\sum_{i=1}^G |\mathbf{o}_i|} \sum_{i=1}^G \sum_{t=1}^{|\mathbf{o}_i|} \underbrace{\left[\frac{\pi_\theta(o_{i,t})}{\pi_{old}(o_{i,t})} \hat{A}_i \cdot \mathbb{I}_{\text{trust}}\left(\frac{\pi_\theta(o_{i,t})}{\pi_{old}(o_{i,t})}, \hat{A}_i\right) + \beta \frac{\pi_{ref}(o_{i,t})}{\pi_\theta(o_{i,t})} - \beta \right]}_{w_{i,t}} \cdot \nabla_\theta \log \pi_\theta(o_{i,t}), \end{aligned} \quad (8)$$

where $\mathbb{I}_{\text{trust}}\left(\frac{\pi_\theta(o_{i,t})}{\pi_{old}(o_{i,t})}, \hat{A}_i\right) = \begin{cases} 0 & \begin{cases} \text{if } \hat{A}_i > 0 \text{ and } \frac{\pi_\theta(o_{i,t})}{\pi_{old}(o_{i,t})} > 1 + \epsilon_h \\ \text{if } \hat{A}_i < 0 \text{ and } \frac{\pi_\theta(o_{i,t})}{\pi_{old}(o_{i,t})} < 1 - \epsilon_l \end{cases} \\ 1 & \text{otherwise} \end{cases}$.

A.2 Proof for Proposition 4.2

Proof. As introduced in Section 4.1, we denote LLM as a composite function $f = f_L \circ f_{L-1} \circ \dots \circ f_1$, where each f_ℓ (with $\ell \in \{1, \dots, L\}$) corresponds to a distinct layer of the network. $\mathbf{a}_{\ell-1}$ denotes the input and \mathbf{a}_ℓ denotes the output of ℓ th layer, and the Jacobian matrix of the ℓ th layer with respect to its input is expressed as $J_\ell := \frac{\partial f_\ell(\mathbf{a}_{\ell-1})}{\partial \mathbf{a}_{\ell-1}}$. For any token $o_{i,t}$, we denote the gradient of GRPO objective with respect to the activations \mathbf{a}_ℓ at ℓ th layer as $\delta_\ell(o_{i,t}) := \nabla_{\mathbf{a}_\ell} J_{GRPO}(o_{i,t})$. According to the rule of backpropagation, we have:

$$\delta_\ell(o_{i,t}) = J_{\ell+1}^\top \delta_{\ell+1}(o_{i,t}) = \prod_{j=\ell+1}^L J_j^\top \cdot \delta_L(o_{i,t}). \quad (9)$$

Note that the gradients of all intermediate layers are back-propagated from the last layer of LLM, thereby we discuss the gradients of the last layer ($\delta_L(o_{i,t})$) first. The last-layer output of an LLM is the logits $\mathbf{a}_L = (a_L^1, a_L^2, \dots, a_L^N)$, which corresponds to a finite vocabulary $\mathcal{V} = \{v^1, v^2, \dots, v^N\}$. The output probability of the corresponding token is calculated through softmax operation:

$$\pi_\theta(v^n) = \frac{e^{a_L^n}}{\sum_{m=1}^N e^{a_L^m}}, \quad \text{for } \forall n \in \{1, 2, \dots, N\}. \quad (10)$$

Given a token $o_{i,t}$, let k denote the index of the logits head corresponding to this token (i.e., $v^k = o_{i,t}$). To obtain the gradient of last layer of LLM, we have:

$$\begin{aligned} \frac{\partial J_{GRPO}(o_{i,t})}{\partial a_L^n} &\stackrel{i}{=} w_{i,t} \cdot \frac{\partial \log \pi_\theta(o_{i,t})}{\partial a_L^n} \\ &\stackrel{ii}{=} w_{i,t} \cdot \sum_{m=1}^N \frac{\partial \log \pi_\theta(o_{i,t})}{\partial \pi_\theta(v^m)} \cdot \frac{\partial \pi_\theta(v^m)}{\partial a_L^n} \\ &\stackrel{iii}{=} w_{i,t} \cdot \frac{\partial \log \pi_\theta(o_{i,t})}{\partial \pi_\theta(v^k)} \cdot \frac{\partial \pi_\theta(v^k)}{\partial a_L^n} = w_{i,t} \cdot \frac{1}{\pi_\theta(v^k)} \cdot \frac{\partial \pi_\theta(v^k)}{\partial a_L^n}. \end{aligned} \quad (11)$$

Here, equality (i) follows from Eq. (8); equality (ii) is obtained by applying the chain rule during backpropagation; and equality (iii) holds because $\partial \log \pi_\theta(o_{i,t}) / \pi_\theta(v^m) = 0$ for all $m \neq k$. Next, we consider the following two cases for the gradient on the logits head a_L^n ($n \in \{1, 2, \dots, N\}$).

Case 1: the logits head corresponds to the sampled token ($n = k$)

$$\begin{aligned} \frac{\partial J_{GRPO}(o_{i,t})}{\partial a_L^k} &= w_{i,t} \cdot \frac{1}{\pi_\theta(v^k)} \cdot \frac{\partial \pi_\theta(v^k)}{\partial a_L^k} \\ &= w_{i,t} \cdot \frac{1}{\pi_\theta(v^k)} \cdot \frac{e^{a_L^k} \cdot \sum_{m=1}^N e^{a_L^m} - e^{2a_L^k}}{(\sum_{m=1}^N e^{a_L^m})^2} \\ &= w_{i,t} \cdot \frac{1}{\pi_\theta(v^k)} \cdot \pi_\theta(v^k) \cdot (1 - \pi_\theta(v^k)) \\ &= w_{i,t} \cdot (1 - \pi_\theta(v^k)). \end{aligned} \quad (12)$$

Case 2: the logits head corresponds to the un-sampled token ($n \neq k$)

$$\begin{aligned} \frac{\partial J_{GRPO}(o_{i,t})}{\partial a_L^n} &= w_{i,t} \cdot \frac{1}{\pi_\theta(v^k)} \cdot \frac{\partial \pi_\theta(v^k)}{\partial a_L^n} \\ &= w_{i,t} \cdot \frac{1}{\pi_\theta(v^k)} \cdot \frac{-e^{a_L^k} \cdot e^{a_L^n}}{(\sum_{m=1}^N e^{a_L^m})^2} \\ &= w_{i,t} \cdot \frac{1}{\pi_\theta(v^k)} \cdot \pi_\theta(v^k) \cdot (-\pi_\theta(v^n)) \\ &= w_{i,t} \cdot (-\pi_\theta(v^n)). \end{aligned} \quad (13)$$

For simplicity, we denote the vector distribution output across the vocabulary as \mathbf{p} , and denote $\mathbf{I}(o_{i,t})$ as the one-hot vector with its only non-zero component at k th position (i.e., the position correspondence to token $o_{i,t}$). We have the following expressions

$$\begin{aligned}\mathbf{p}(o_{i,t}) &= (\pi_\theta(v^1), \pi_\theta(v^2), \dots, \pi_\theta(v^N)) \in \mathcal{R}^N \\ \mathbf{I}(o_{i,t}) &= (0, 0, \dots, \underbrace{1}_{k\text{th}}, \dots, 0) \in \mathcal{R}^N.\end{aligned}\quad (14)$$

Combining Eq. (12) and Eq. (13), and utilizing the notation defined in Eq. (14), we obtain:

$$\delta_L(o_{i,t}) = \nabla_{\mathbf{a}_L} J_{GRPO}(o_{i,t}) = w_{i,t} \cdot (\mathbf{I}(o_{i,t}) - \mathbf{p}(o_{i,t})). \quad (15)$$

Considering the lower bound for the gradient norm, we have:

$$\begin{aligned}\|\delta_L(o_{i,t})\| &= |w_{i,t}| \cdot \|\mathbf{p}(o_{i,t}) - \mathbf{I}(o_{i,t})\| \\ &= |w_{i,t}| \cdot \sqrt{(1 - \pi_\theta(v^k))^2 + \sum_{n \neq k}^N \pi_\theta(v^n)^2} \\ &\geq |w_{i,t}| \cdot \sqrt{(1 - \pi_\theta(v^k))^2 + \frac{1}{N-1} \left(\sum_{n \neq k}^N \pi_\theta(v^n)\right)^2} \\ &= |w_{i,t}| \cdot \sqrt{(1 - \pi_\theta(v^k))^2 + \frac{1}{N-1} (1 - \pi_\theta(v^k))^2} \\ &= |w_{i,t}| \cdot \sqrt{\frac{N}{N-1}} (1 - \pi_\theta(o_{i,t})),\end{aligned}\quad (16)$$

where the inequality follows from the Cauchy-Schwarz inequality. The equality holds holding if and only if $\pi_\theta(v^n)$ is uniformly distributed for all $n \neq k$.

By substituting Eq.(16) into Eq.(9), we obtain:

$$\begin{aligned}\|\delta_\ell(o_{i,t})\| &= \left\| \prod_{j=\ell+1}^L J_j^\top \cdot \delta_L(o_{i,t}) \right\| \\ &\geq \prod_{j=\ell+1}^L \sigma_{\min}(J_j^\top) \cdot \|\delta_L(o_{i,t})\| \\ &\stackrel{ii}{\geq} \prod_{j=\ell+1}^L c_j \cdot \|\delta_L(o_{i,t})\| \\ &\stackrel{iii}{\geq} \prod_{j=\ell+1}^L c_j \cdot |w_{i,t}| \cdot \sqrt{\frac{N}{N-1}} (1 - \pi_\theta(v^k)),\end{aligned}\quad (17)$$

where inequality (i) follows from the variational characterization of singular values, inequality (ii) is a consequence of Assumption 4.1, and inequality (iii) results from Eq. (16).

Next, considering an alternative direction, we derive an upper bound for the gradient norm:

$$\begin{aligned}\|\delta_L(o_{i,t})\| &= |w_{i,t}| \cdot \sqrt{(1 - \pi_\theta(v^k))^2 + \sum_{n \neq k}^N \pi_\theta(v^n)^2} \\ &\leq |w_{i,t}| \cdot \sqrt{(1 - \pi_\theta(v^k))^2 + \sum_{n \neq k}^N \pi_\theta(v^n)^2 + 2 \sum_{n, m \neq k, n < m}^N \pi_\theta(v^n) \pi_\theta(v^m)} \\ &= |w_{i,t}| \cdot \sqrt{(1 - \pi_\theta(v^k))^2 + \left(\sum_{n \neq k}^N \pi_\theta(v^n)\right)^2} \\ &= |w_{i,t}| \cdot \sqrt{(1 - \pi_\theta(v^k))^2 + (1 - \pi_\theta(v^k))^2} \\ &= |w_{i,t}| \cdot \sqrt{2} (1 - \pi_\theta(o_{i,t})),\end{aligned}\quad (18)$$

where the inequality holds because $\pi_\theta(v^n) \geq 0$ for all $n \in 1, 2, \dots, N$. The equality is achieved if and only if there exists an index m such that $\pi_\theta(v^m) = 1 - \pi_\theta(v^k)$ and $\pi_\theta(v^n) = 0$ for all $n \neq m$ and $n \neq k$.

Similarly, substituting Eq.(18) into Eq.(9), we have

$$\begin{aligned}
\|\delta_\ell(o_{i,t})\| &= \left\| \prod_{j=\ell+1}^L J_j^\top \cdot \delta_L(o_{i,t}) \right\| \\
&\leq \prod_{j=\ell+1}^L \sigma_{\max}(J_j^\top) \cdot \|\delta_L(o_{i,t})\| \\
&\leq \prod_{j=\ell+1}^L d_j \cdot \|\delta_L(o_{i,t})\| \\
&\leq \prod_{j=\ell+1}^L d_j \cdot |w_{i,t}| \cdot \sqrt{2} (1 - \pi_\theta(v^k)),
\end{aligned} \tag{19}$$

where the inequalities hold for the same reasons as in Eq. (17). Together, Eqs. (17) and (19) establish the result of Proposition 4.2.

B Hyperparameter Settings

As described in Section 4.2, our proposed *Advantage Reweighting* and *Lopti* require only minor modifications to the existing GRPO training framework. Our implementation is built upon the `verl` library[‡] [44]. The key hyperparameter configurations for GRPO training are detailed in Table 2. Note that we adopt the ‘clip higher’ technique from DAPO [9] to stabilize entropy and mitigate entropy collapse. All other hyperparameters adhere to the default settings provided by `verl`.

The hyperparameter configurations specific to *Advantage Reweighting* and *Lopti* are summarized in Table 3. As reported in Section 5, while the joint application of the two techniques generally yields improved results for the K&K Logic Puzzle dataset, this is not the case for the Math dataset. Consequently, using either technique individually is recommended for the math-related dataset. For consistency, the same seed is used across all experiments. We save a checkpoint every 20 RL steps, and all evaluation accuracies reported on the test set in this paper are averaged over the last three checkpoints. The detailed implementation can be found in our code.

Table 2: Key hyperparameters for GRPO training, with the corresponding variable names in the `verl` configuration indicated in brackets.

Hyperparameter	Value	
	K&K	Math
Rollout-related		
Sampling temperature (temperature)	0.7	1.0
Question num per batch (ppo_mini_batch_size)	64	128
Answer num per question (rollout.n)	8	
Max tokens num per response (max_response_length)	4096	
Training-related		
Update batch size (ppo_micro_batch_size)	256	512
Optimizer (optim.type)	adamw	
Learning rate (optim.lr)	1e-6	
KL divergence coefficient (kl_loss_coef)	0.001	
Lower clipping threshold (clip_ratio_low)	0.2	
Upper clipping threshold (clip_ratio_high)	0.24	

Table 3: Hyperparameter settings for *Advantage Reweighting* and *Lopti*.

Hyperparameter	Value	
	K&K	Math
Advantage Reweighting (α)	0.3	0.1
Lopti (η)	0.5	0.5
Joint operation for better results	True	False

[‡]<https://github.com/volcengine/verl>

C Experimental Details

C.1 Task Description

C.1.1 K&K Logic Puzzle

As introduced in Section 5.1, the K&K logic puzzles involve a fictional scenario where inhabitants of an island are either Knights, who always tell the truth, or Knaves, who always lie. The objective of the LLMs is to determine the identity of each inhabitant (Knight or Knave) based on a set of statements they make about themselves and others. Following Logic-RL [38], we utilize the LLMs after instruction fine-tuning (Qwen2.5-3B-Instruct and Qwen2.5-7B-Instruct-1M) as starting point. The prompt specifically designed for the LLMs is as follows.

Prompt

```
system\n You are a helpful assistant. The assistant first thinks about the reasoning process in the mind and then provides the user with the answer. The reasoning process and answer are enclosed within <think> </think> and<answer> </answer> tags, respectively, i.e., <think> reasoning process here </think><answer> answer here </answer>. Now the user asks you to solve a logical reasoning problem. After thinking, when you finally reach a conclusion, clearly state the identity of each character within <answer> </answer> tags. i.e., <answer> (1) Zoey is a knight\n (2) ... </answer>.\n\n user\n {problem}\n\n assistant\n <think>
```

To encourage LLMs to exhibit chain-of-thought (CoT) reasoning, Logic-RL [38] designs a reward function consisting of two components, as outlined in Table 4. The output format is deemed completely correct if LLMs include CoT reasoning enclosed within <think></think> tags and the final answer enclosed within <answer></answer> tags.

Table 4: Reward design for K&K Logic Puzzle proposed in Logic-RL [38]

	Format Reward	Answer Reward
Completely Correct	1	2
Patially Correct	-1	-1.5
Completely Wrong	-1	-2

For the K&K Logic Puzzle dataset, the number of players (ranging from 3 to 7) can be adjusted to control the difficulty level, with a greater number of players resulting in higher difficulty. To provide an intuitive illustration, we present an easy example with 3 players and a challenging example with 7 players below. Without utilizing curriculum learning, we directly train the LLMs on the mixed training set for a total of 5 epochs.

An Example of K&K Puzzle with 3 people

Problem:

A very special island is inhabited only by knights and knaves. Knights always tell the truth, and knaves always lie. You meet 3 inhabitants: Alexander, Lily, and Samuel. Alexander remarked, "Lily is a knave or Lily is a knight". In a statement by Lily: "Samuel is a knight if and only if Lily is a knight". Samuel was heard saying, "Lily is a knight". So who is a knight and who is a knave?

Example Reasoning Process:

- Assume Alexander is a knight. No contradiction is found in their claim that Lily is a knave or Lily is a knight.
- Assume Lily is a knight. No contradiction is found in their claim that Samuel is a knight if and only if Lily is a knight.
- Assume Samuel is a knight. No contradiction is found in their claim that Lily is a knight.

Standard Solution:

(1) Alexander is a knight, (2) Lily is a knight, (3) Samuel is a knight

An Example of K&K Puzzle with 7 people

Problem:

A very special island is inhabited only by knights and knaves. Knights always tell the truth, and knaves always lie. You meet 7 inhabitants: Harper, Emma, Mia, Luke, Alexander, David, and Ethan. As Harper put it, "David is not a knight". In Emma's words: "David is a knight". Mia said that If Emma is a knight then Emma is a knave. Luke said, "If Alexander is a knave then Emma is a knight." Alexander was heard saying, "If David is a knight then Harper is a knave". "Alexander is not a knight" - David. "Harper is a knight," Ethan mentioned. So who is a knight and who is a knave?

Example Reasoning Process:

- Assume Harper is a knight. No contradiction is found in their claim that David is not a knight.
- David cannot be a knight, because this would contradict the claim of Harper that David is not a knight.
- Assume David is a knave. No contradiction is found in their false claim that Alexander is not a knight.
- Assume Alexander is a knight. No contradiction is found in their claim that If David is a knight then Harper is a knave.
- Emma cannot be a knight, because this would contradict the claim of their own that David is a knight.
- Assume Emma is a knave. No contradiction is found in their false claim that David is a knight.
- Assume Mia is a knight. No contradiction is found in their claim that If Emma is a knight then Emma is a knave.
- Assume Luke is a knight. No contradiction is found in their claim that If Alexander is a knave then Emma is a knight.
- Assume Ethan is a knight. No contradiction is found in their claim that Harper is a knight.

Standard Solution:

(1) Harper is a knight (2) Emma is a knave (3) Mia is a knight (4) Luke is a knight (5) Alexander is a knight (6) David is a knave (7) Ethan is a knight

The detailed training records for Qwen2.5-3B-Instruct and Qwen2.5-7B-Instruct-1M are presented in Figure 7 and Figure 8, respectively. In addition to the points discussed in Section 5.1, it is worth noting that our *Advantage Reweighting* and *Lopti* approaches slightly increase the response length while significantly reducing the gradient norm compared to the naive GRPO. Both observations empirically suggest that the RL training process is further stabilized.

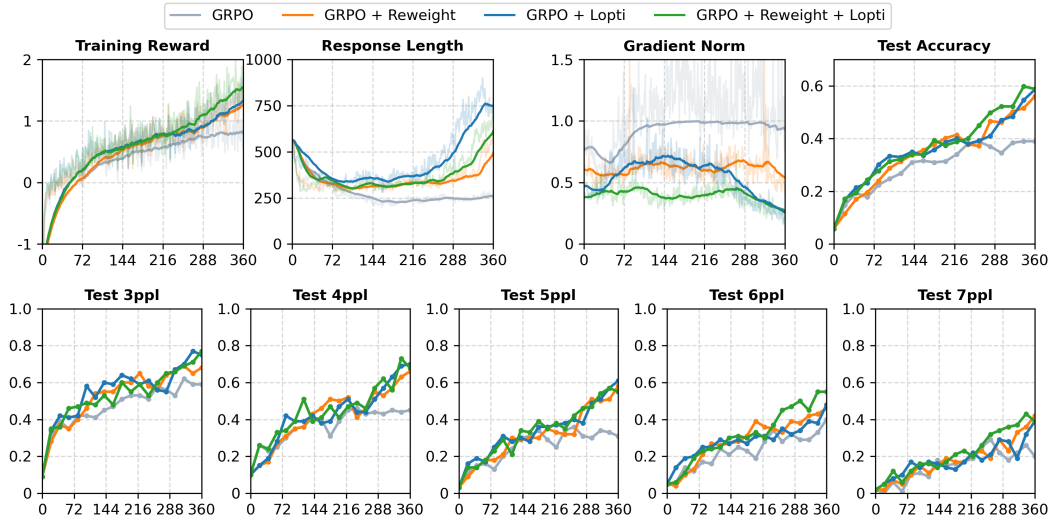


Figure 7: Experimental records of Qwen2.5-3B-Instruct trained with GRPO on the K&K Logic Puzzle dataset. The training curve is smoothed through exponential moving average with coefficient of 0.95.

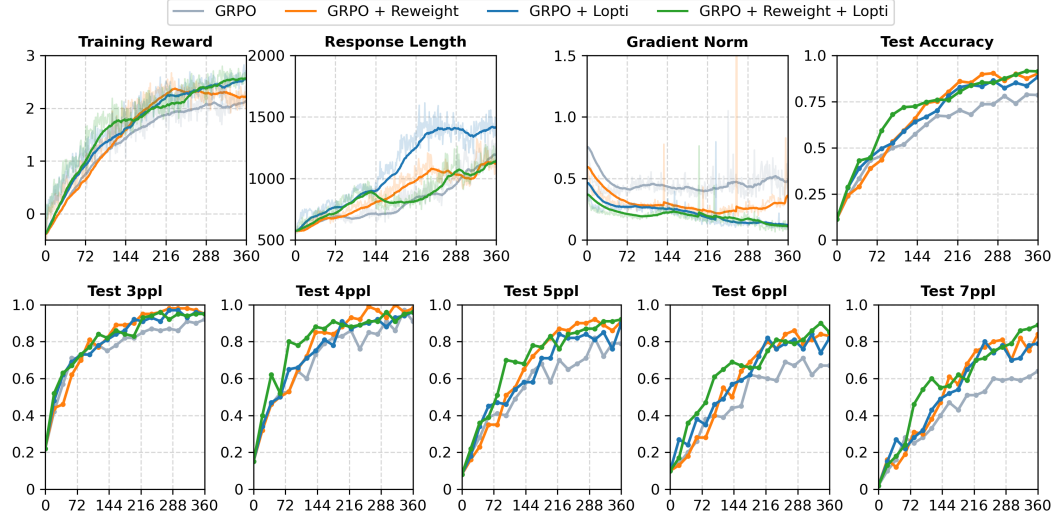


Figure 8: Experimental records of Qwen2.5-7B-Instruct-1M trained with GRPO on the K&K Logic Puzzle dataset.

For the six categories of inference-related words used in the linguistic analysis, the detailed word lists are provided in Table 5. It is important to note that for the nouns and verbs listed in the table, their conjugated forms are also included in the analysis. Specifically, we account for the plural forms of nouns as well as the past tense and past participle forms of verbs. Additionally, uppercase and lowercase letters are treated equivalently.

Table 5: Six categories of inference-related words associated with LLMs’ performance on the K&K Logic Puzzles dataset.

Category	Words (Nouns and verbs include their conjugated forms)
Analysis	‘analyze’, ‘consider’, ‘look at’, ‘check’, ‘examine’
Statement	XXX’s ‘statement’
Causal Indicator	‘since’, ‘because’, ‘due to’, ‘given that’
Conclusion Indicator	‘so’, ‘thus’, ‘hence’, ‘as a result’, ‘consequently’, ‘therefore’
Assumption	‘assume’, ‘if...then...’
Assertion	‘must be’, ‘definite’

C.1.2 Math Dataset

As discussed in Section 5.2, we perform additional experiments on two math-related datasets, DSR-Uniform and ORZ. Consistent with the majority of prior studies, we use Qwen2.5-7B as the starting point. It is important to note that Qwen2.5-7B undergoes no post-training. This setup is therefore referred to as a "cold-start" and denoted as RL-Zero [2]. No instruction-following templates are employed; instead, we use the following straightforward prompt.

Prompt

{problem} Let’s think step by step and output the final answer within `\boxed{ }`.

LLMs that have not undergone post-training typically exhibit poor performance in adhering to specific output formats. As a result, format-related points were not included during training. Additionally, math problems are generally not partially correct, making a binary reward sufficient for evaluating the LLMs’ output. Specifically, a reward of 1 is assigned when LLMs produce the correct answer, and 0 otherwise.

The detailed experimental results for the DSR-Uniform and ORZ datasets are presented in Figure 9 and Figure 10, respectively. Notably, the training curve for DSR-Uniform demonstrates a continual learning trend, with the reward progressively increasing over time. In contrast, this is not observed for ORZ, where the reward converges rapidly within 100 steps. However, the test accuracy curves for both datasets converge to a stable value within 100 steps, after which they exhibit only minor fluctuations. Despite these patterns, the improvements achieved by our proposed methods, *Advantage Reweighting* and *Lopti*, remain clearly observable.

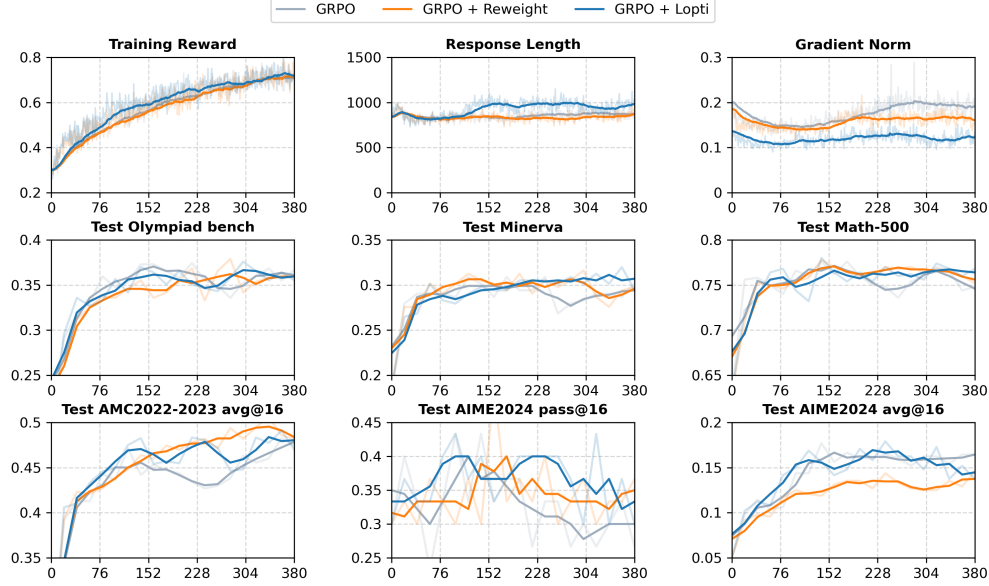


Figure 9: Experimental records of Qwen2.5-7B trained with GRPO on DSR-uniform dataset. The training curve is smoothed through exponential moving average with coefficient of 0.95, and the testing curve is smoothed with a window size of 3.

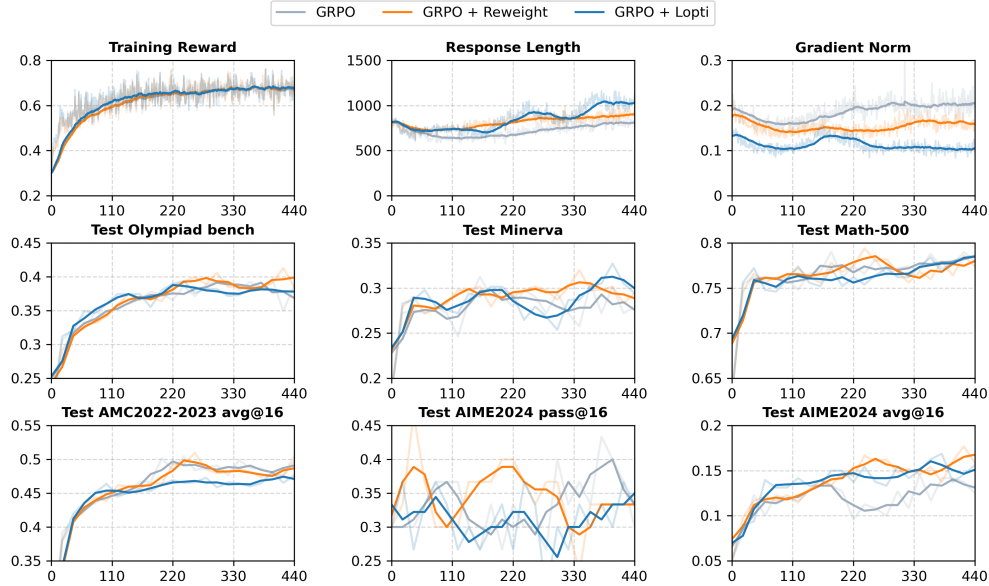


Figure 10: Experimental records of Qwen2.5-7B trained with GRPO on ORZ dataset.

C.2 Computational Costs

Our experiments are conducted on a single machine equipped with an AMD EPYC 7V13 64-Core CPU and four NVIDIA A100 80GB PCIe GPUs. The experiments on the K&K Logic Puzzle dataset require approximately 16–22 hours to complete (excluding testing during the training process), while those on the math-related dataset take around 37–48 hours.

The *Advantage Reweighting* involves only recalculating the advantage of tokens, with a time overhead in the range of milliseconds. However, this efficiency does not apply to *Lopti*, as it splits the tokens in a batch into two groups and performs updates twice. Consequently, the updating process requires twice the amount of time, as detailed in Table 6.

Table 6: Computational cost comparison of *Lopti* operation over the first 50 training steps on K&K Logic Puzzle Dataset.

Procedure	Time (s)/step			
	Qwen2.5-3B-Instruct w/o Lopti	Qwen2.5-3B-Instruct w/ Lopti	Qwen2.5-7B-Instruct-1M w/o Lopti	Qwen2.5-7B-Instruct-1M w/ Lopti
Sampling	25.4	27.8	61.4	116.8
Training	17.6	35.3	68.5	69.3
Others	2.4	2.8	10.3	10.2
Total	45.4	65.9	140.2	196.3

D Additional Experimental Results on REINFORCE++

In addition to GRPO, our proposed methods, *Advantage Reweighting* and *Lopti*, are also well-adapted to other Policy Gradient-based RL algorithms. In this section, we extend our methods to REINFORCE++ [46], a widely recognized algorithm that builds upon the conventional REINFORCE [53] while incorporating various stabilization techniques introduced by PPO [16]. We first provide an introduction to the REINFORCE++ in Appendix D.1 and subsequently present the experimental results in Appendix D.2.

D.1 REINFORCE++

Similar to GRPO, REINFORCE++ also eliminates the need for a value model, thereby reducing computational costs compared to PPO. The key differences between GRPO and REINFORCE++ lie in how they *estimate the advantage* and *constrain the distance between the RL-trained model and the initial (or reference) model*. GRPO estimates the advantage based on the difference between the reward and the group-relative expected return, incorporating the KL constraint directly into the objective function (cf. Section 3 for details). In contrast, REINFORCE++ does not emphasize the concept of ‘group’ under the same prompt. Instead, it estimates the advantage directly from the reward and treats the KL constraint as a penalty term added to the reward. Specifically, REINFORCE++ estimates the advantage as follows:

$$\hat{A}_{i,t} = \frac{\hat{A}_{i,t}^{R++} - \mu_A}{\sigma_A} \quad \text{with} \quad \hat{A}_{i,t}^{R++} = r(\mathbf{q}, \mathbf{o}_i) - \beta \cdot \sum_{j=t}^T \mathbb{D}_{\text{KL}} [\pi_{\theta}(\mathbf{o}_{i,j}) \| \pi_{\text{ref}}(\mathbf{o}_{i,j})], \quad (20)$$

where μ_A and σ_A represent the mean and standard deviation of the advantages of all tokens within the RL-sampled batch, respectively. The KL divergence term is computed using the k1 estimation [52]: $\mathbb{D}_{\text{KL}} [\pi_{\theta}(\mathbf{o}_{i,j}) \| \pi_{\text{ref}}(\mathbf{o}_{i,j})] = \pi_{\theta}(\mathbf{o}_{i,j}) / \pi_{\text{ref}}(\mathbf{o}_{i,j})$. The optimization objective of REINFORCE++ is:

$$J_{R++}(\theta) = \mathbb{E}_{\mathbf{q} \sim \mathcal{D}, \{\mathbf{o}_i\}_{i=1}^G \sim \pi_{\text{old}}} \frac{1}{\sum_{i=1}^G |\mathbf{o}_i|} \sum_{i=1}^G \sum_{t=1}^{|\mathbf{o}_i|} \left\{ \min \left[r_{i,t}(\theta) \hat{A}_{i,t}, \text{clip}(r_{i,t}(\theta); 1 - \epsilon_l, 1 + \epsilon_h) \hat{A}_{i,t} \right] \right\} \quad (21)$$

with $r_{i,t}(\theta) = \frac{\pi_{\theta}(\mathbf{o}_{i,t} | \mathbf{q}, \mathbf{o}_{i,<t})}{\pi_{\text{old}}(\mathbf{o}_{i,t} | \mathbf{q}, \mathbf{o}_{i,<t})}$.

D.2 Experiments on K&K Logic Puzzle

Similar to the experiments conducted with GRPO, we validate two base models as starting points: Qwen2.5-3B-Instruct and Qwen2.5-7B-Instruct-1M. All hyperparameters of REINFORCE++ are kept consistent with those used for GRPO, as described in Appendix B. The only difference is that, on the K&K Logic Puzzle dataset, the optimal hyperparameter setting for *Advantage Reweighting* is $\alpha = 0.1$ for REINFORCE++, and $\alpha = 0.3$ for GRPO.

The evaluation results on the test set are reported in Table 7. Notably, the performance of naive REINFORCE++ is slightly worse than that of naive GRPO (cf. Figure 4). This observation aligns with the findings of Xiong et al. [11], as the advantage normalization method in REINFORCE++ may introduce unnecessary bias toward entirely incorrect responses on overly difficult prompts. Nevertheless, the improvements achieved by our proposed methods, *Advantage Reweighting* and *Lopti*, remain significant. For more details on the training process, please refer to the records presented in Figure 11 and Figure 12.

Table 7: Experimental results of REINFORCE++ on the K&K Logic Puzzles dataset. For *Advantage Reweight*, $\alpha = 0.1$, and for *Lopti*, $\eta = 0.5$. The evaluation accuracy on the test set are averaged over the last three checkpoints to mitigate randomness.

Model	Difficulty by Number of People					
	3	4	5	6	7	Avg.
Qwen2.5-3B-Instruct	0.09	0.10	0.03	0.05	0.02	0.06
REINFORCE++	0.37	0.31	0.20	0.21	0.06	0.23
REINFORCE++ with Reweight	0.53	0.44	0.31	0.26	0.14	0.34 ($\uparrow 46.1\%$)
REINFORCE++ with Lopti	0.47	0.36	0.26	0.26	0.12	0.29 ($\uparrow 27.8\%$)
REINFORCE++ with Reweight & Lopti	0.61	0.49	0.38	0.34	0.21	0.41 ($\uparrow 76.5\%$)
Qwen2.5-7B-Instruct-1M	0.22	0.15	0.08	0.10	0.02	0.11
REINFORCE++	0.68	0.72	0.54	0.42	0.43	0.56
REINFORCE++ with Reweight	0.81	0.77	0.66	0.62	0.48	0.67 ($\uparrow 19.7\%$)
REINFORCE++ with Lopti	0.89	0.85	0.71	0.66	0.51	0.72 ($\uparrow 29.7\%$)
REINFORCE++ with Reweight & Lopti	0.87	0.88	0.81	0.71	0.69	0.79 ($\uparrow 41.9\%$)

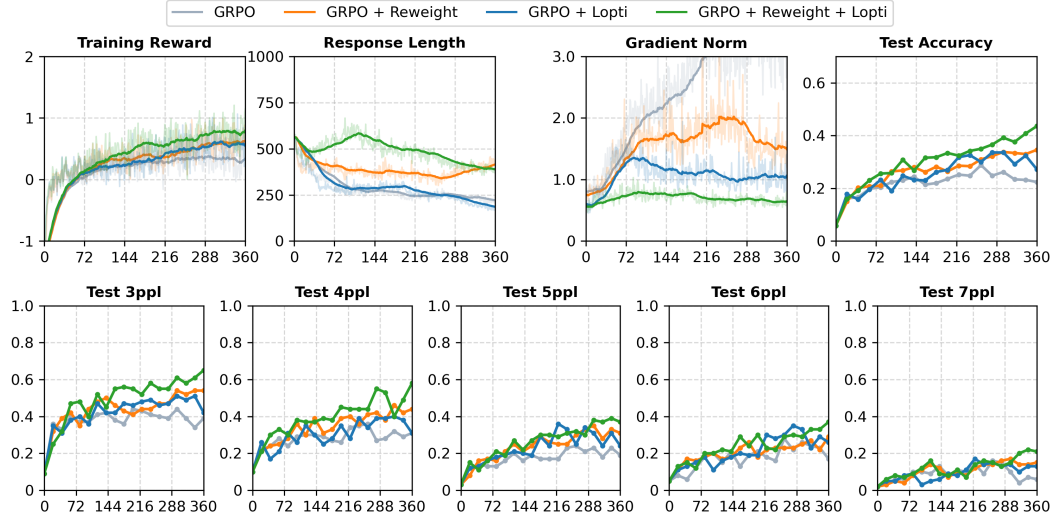


Figure 11: Experimental records of Qwen2.5-3B-Instruct trained with REINFORCE++ on the K&K Logic Puzzle dataset. The training curve is smoothed through exponential moving average with coefficient of 0.95.

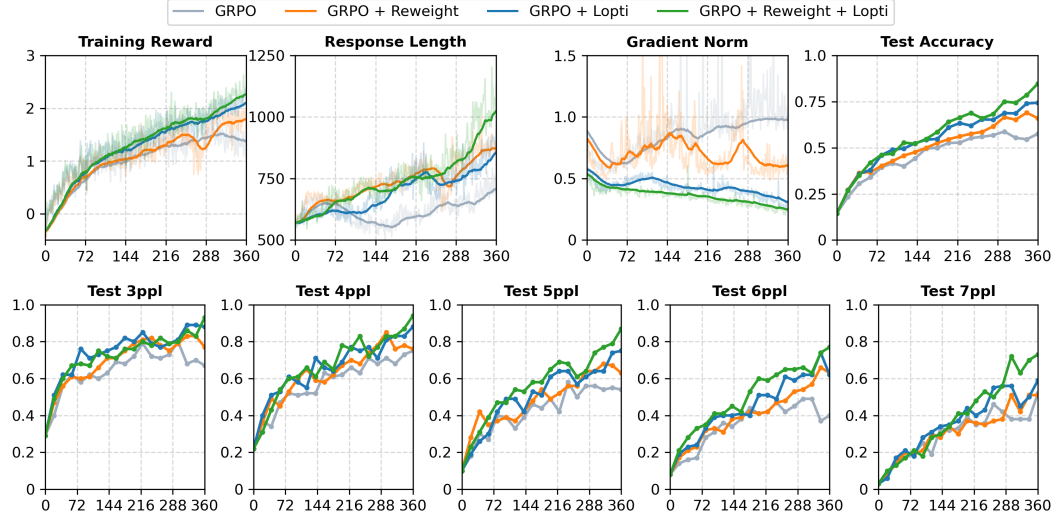


Figure 12: Experimental records of Qwen2.5-7B-Instruct-1M trained with REINFORCE++ on the K&K Logic Puzzle dataset.

E Limitations

One limitation of our study lies in the additional computational overhead introduced by *Lopti*. As detailed in Appendix C.2, the updating process requires twice the amount of time as it splits the tokens in a batch into two groups and performs updates twice. However, we also propose an alternative method, *Advantage Reweighting*, which incurs negligible computational cost while achieving even greater improvements on the math-related dataset compared to *Lopti*.